

Supporting Information

Valence-to-core X-ray emission spectroscopy to resolve the size-dependent valence electronic structure of Pt nanoparticles

David P. Dean^a, Gaurav S. Deshmukh^a, Christopher K. Russell^a, Kuixin Zhu^b, Christina W. Li^b, Jeffrey P. Greeley^a, Denis Leshchev^{c,}, Eli Stavitski^{c,*}, Jeffrey T. Miller^{a,*}*

^aDavidson School of Chemical Engineering, Purdue University, West Lafayette, IN 47907, USA

^bDepartment of Chemistry, Purdue University, West Lafayette, IN 47907, USA

^cBrookhaven National Laboratory NSLS-II, Upton, NY 11973, USA

*Corresponding authors:

jeffrey-t-miller@purdue.edu

dleshev@bnl.gov

stavitski@bnl.gov

The lattice strain for surface, subsurface, and bulk atoms of Pt-314 is calculated. The x-, y-, and z-components of strain for the surface, subsurface, and bulk atoms of Pt (designed in the nanoparticle in Figure S1) are calculated and tabulated in Table S1, Table S2, and Table S3. The strain (ϵ_{ij}) for a bond between two atoms having a bond length of a_{ij} in a lattice with a lattice constant of a_{Pt} is calculated as follows:

$$\epsilon_{ij} = \frac{a_{ij} - a_{Pt}}{a_{Pt}}$$

The components of strain are calculated as follows:

$$\epsilon_{ij}^x = \epsilon_{ij}(\cos(\theta_{xy}) + \sin(\theta_{xz}))$$

$$\epsilon_{ij}^y = \epsilon_{ij}(\sin(\theta_{xy}) + \cos(\theta_{yz}))$$

$$\epsilon_{ij}^z = \epsilon_{ij}(\cos(\theta_{xz}) + \sin(\theta_{yz}))$$

Where θ_{xy} , θ_{yz} , θ_{xz} represent the angles made by the bonds with the x-axis (in the xy plane), y-axis (in the yz-plane), z-axis (in the xz-plane) respectively.

From the tabulated values of strain, it is evident that the sub-surface atom experiences an unusually large magnitude of compressive strain (~47%) in the axial (or x-) direction, which neither the surface nor the bulk atom experience.

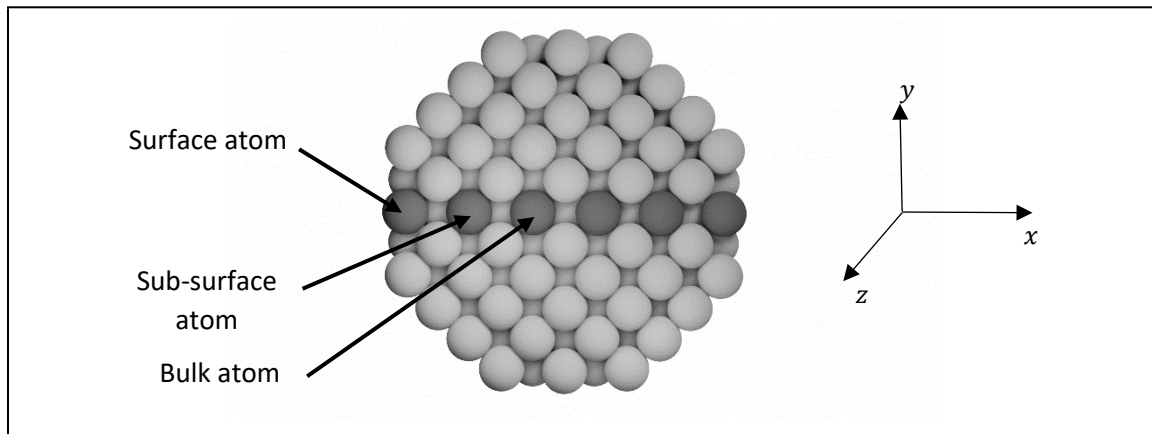


Figure S1: Cross section of the Pt-314 nanoparticle with the surface, sub-surface, and bulk atoms annotated.

Table S1: Bond lengths and angles for bonds of the surface atom with its 8 neighbors and calculated strains.

	$a_{ij}(\text{\AA})$	$\theta_{xy}(\text{\textcircled{C}})$	$\theta_{yz}(\text{\textcircled{C}})$	$\theta_{xz}(\text{\textcircled{C}})$	ϵ_{ij}	ϵ_{ij}^x	ϵ_{ij}^y	ϵ_{ij}^z
Surface atom	2.75	90.0	45.0	0.0	-0.024	0.000	-0.041	-0.016
	2.75	90.0	45.0	0.0	-0.024	0.000	-0.041	-0.016
	2.75	90.0	45.0	0.0	-0.024	0.000	-0.041	-0.016
	2.75	90.0	45.0	0.0	-0.024	0.000	-0.041	-0.016
	2.83	0.0	90.0	45.7	0.001	0.002	0.000	0.001
	2.83	0.0	90.0	45.7	0.001	0.002	0.001	0.001
	2.83	44.3	0.0	90.0	0.001	0.002	0.002	0.000
	2.83	44.3	0.0	90.0	0.001	0.002	0.001	0.000
Net strain						0.010	-0.160	-0.062

Table S2: Bond lengths and angles for bonds of the sub-surface atom with its 12 neighbors and calculated strains.

	$a_{ij}(\text{\AA})$	$\theta_{xy}(\text{\textcircled{C}})$	$\theta_{yz}(\text{\textcircled{C}})$	$\theta_{xz}(\text{\textcircled{C}})$	ϵ_{ij}	ϵ_{ij}^x	ϵ_{ij}^y	ϵ_{ij}^z
Sub-Surface atom	2.89	90.0	45.0	0.0	0.025	0.000	0.042	0.018
	2.89	90.0	45.0	0.0	0.025	0.000	0.042	0.018
	2.89	90.0	45.0	0.0	0.025	0.000	0.042	0.018
	2.89	90.0	45.0	0.0	0.025	0.000	0.042	0.018
	2.76	0.0	90.0	43.8	-0.023	-0.039	0.000	-0.023
	2.76	0.0	90.0	43.8	-0.023	-0.039	0.000	-0.023

	2.69	0.0	90.0	42.8	-0.047	-0.079	0.000	-0.047
	2.69	0.0	90.0	42.8	-0.047	-0.079	0.000	-0.047
	2.69	47.2	0.0	90.0	-0.047	-0.079	-0.081	0.000
	2.69	47.2	0.0	90.0	-0.047	-0.079	-0.081	0.000
	2.76	46.2	0.0	90.0	-0.023	-0.039	-0.040	0.000
	2.76	46.2	0.0	90.0	-0.023	-0.039	-0.040	0.000
Net strain						-0.472	-0.074	-0.068

Table S3: Bond lengths and angles for bonds of the bulk atom with its 12 neighbors and calculated strains.

	$a_{ij}(\text{\AA})$	$\theta_{xy}(\text{\textcircled{C}})$	$\theta_{yz}(\text{\textcircled{C}})$	$\theta_{xz}(\text{\textcircled{C}})$	ϵ_{ij}	ϵ_{ij}^x	ϵ_{ij}^y	ϵ_{ij}^z
Bulk atom	2.79	90.0	45.0	0.0	-0.010	0.000	-0.017	-0.007
	2.79	90.0	45.0	0.0	-0.010	0.000	-0.017	-0.007
	2.79	90.0	45.0	0.0	-0.010	0.000	-0.017	-0.007
	2.79	90.0	45.0	0.0	-0.010	0.000	-0.017	-0.007
	2.82	0.0	90.0	45.0	0.000	0.000	0.000	0.000
	2.82	0.0	90.0	45.0	0.000	0.000	0.000	0.000
	2.79	0.0	90.0	44.5	-0.011	-0.019	0.000	-0.011
	2.79	0.0	90.0	44.5	-0.011	-0.019	0.000	-0.011
	2.82	45.0	0.0	90.0	0.000	0.000	0.000	0.000
	2.82	45.0	0.0	90.0	0.000	0.000	0.000	0.000
	2.79	45.5	0.0	90.0	-0.011	-0.019	-0.019	0.000
	2.79	45.5	0.0	90.0	-0.011	-0.019	-0.019	0.000

Net strain	-0.076	-0.106	-0.050
------------	--------	--------	--------

A detailed description for the theoretical calculations of X-ray absorption and emission spectra for solids based on the energy-band model is provided in Kotani & Shin.¹ Further, Bukowski et al.² apply this theory to calculate resonant inelastic X-ray scattering (RIXS) planes of Pt and Pt-based alloy catalysts from partial density of states (pDOS) obtained using density functional theory (DFT). They use the following equation to calculate intensity of RIXS planes (F) based on the incident energy (Ω), emission energy (ω), partial density of occupied states (ρ_d), partial density of unoccupied states (ρ_d'), and core-hole broadening (Γ_n).

$$F(\Omega, \omega) = \int_{-\infty}^0 d\epsilon \frac{\rho_d(\epsilon) \rho_d'(\epsilon + \Omega - \omega)}{(\epsilon - \omega)^2 + \frac{\Gamma_n^2}{4}}$$

We formulate our approach to calculate XES intensities from DFT-predicted Pt pDOS based on this previous analysis. In contrast to RIXS, in which the excited electron transitions to an unoccupied state, XES involves transition of the excited electron to the continuum. The intensity can therefore be assumed to be independent of the incident energy and the unoccupied states, and we get the following equation for the intensity as a function of the emission energy.

$$F(\omega) = \int_{-\infty}^0 d\epsilon \frac{\rho_d(\epsilon)}{(\epsilon - \omega)^2 + \frac{\Gamma_n^2}{4}}$$

We utilize the above equation to calculate intensities in a range of emission energies (from -10 eV to 5 eV) for the four Pt octahedral nanoparticle clusters whose pDOS we have evaluated using DFT and plot them in Figure S2. The core-hole broadening term is assumed to be 5.41 eV based on previous analyses.^{2,3} The intensities are scaled such that the maximum intensity for each nanoparticle is the same and equal to the maximum intensity of Pt-314. We find, similar to the experimental XES spectra, that the peaks skew toward the Fermi level with decreasing nanoparticle size (and increasing dispersion). Note that the calculated intensities have smaller peak shifts compared to the experimental intensities since the range of nanoparticle sizes for which DFT calculations are performed is smaller than the range of sizes of the experimental

samples. The peak positions of the intensities and full widths at half maxima (FWHM) are calculated and listed in Table S4 and Table S5 respectively. The FWHM are similar in magnitude to the experimental measurements and are found to decrease slightly with decrease in nanoparticle size, a trend observed in the measurements as well. We also calculate the upper edges (see Table S6) and find that they follow a linear relationship, as observed for the experimental upper edge measurements (plotted in Figure S3).

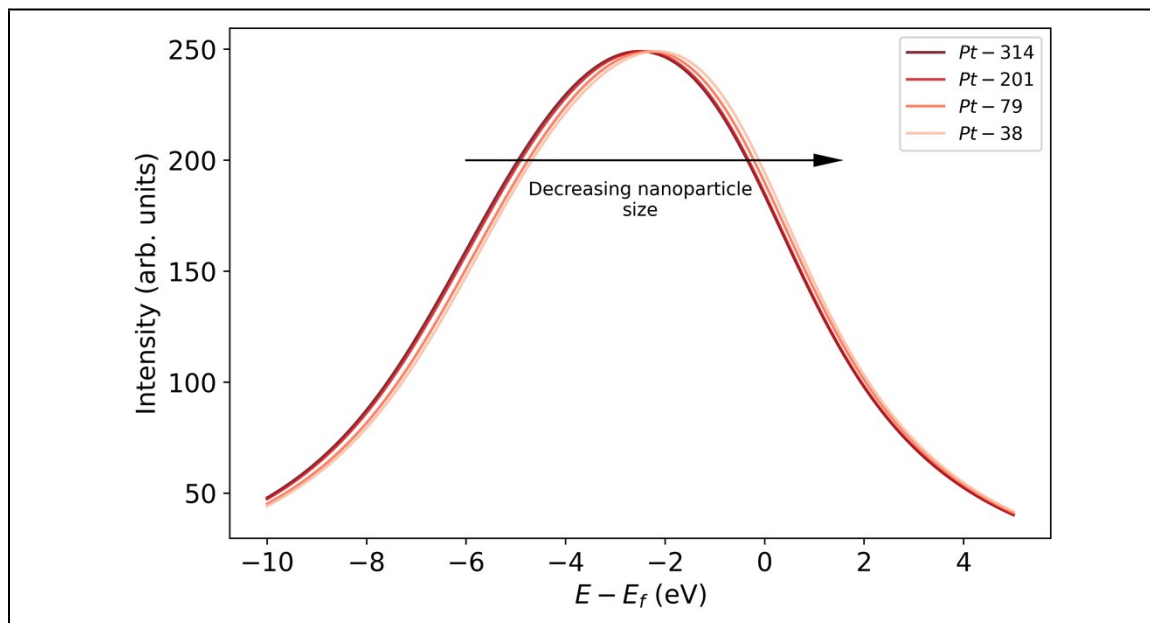


Figure S2: Calculated XES intensities of four nanoparticles—Pt-38, Pt-79, Pt-201, and Pt-314. The spectra are colored (from light to dark) in increasing order of nanoparticle size.

Table S4: Calculated XES peak positions for four octahedral nanoparticle clusters. The resolution of the calculated pDOS based on which these values are estimated is 0.01 eV.

Nanoparticle	Peak position (eV)
Pt-314	-2.52
Pt-201	-2.46
Pt-79	-2.31
Pt-38	-2.16

Table S5: Calculated FWHM for four octahedral nanoparticle clusters. The resolution of the calculated pDOS based on which these values are estimated is 0.01 eV.

Nanoparticle	FWHM (eV)
Pt-314	8.15
Pt-201	8.12

Pt-79	8.05
Pt-38	8.03

Table S6: Calculated upper edges for four octahedral nanoparticle clusters. The resolution of the calculated pDOS based on which these values are estimated is 0.01 eV.

Nanoparticle	Upper edge (eV)
Pt-314	1.28
Pt-201	1.29
Pt-79	1.38
Pt-38	1.44

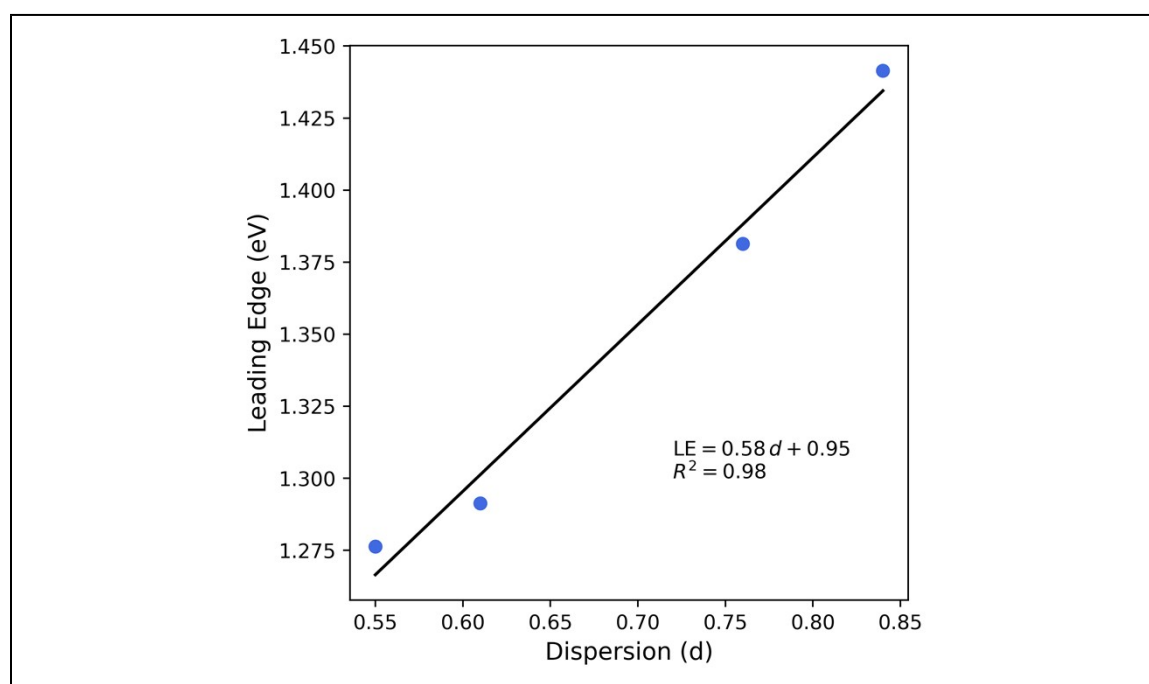


Figure S3: Plot of calculated upper (leading) edges against dispersion for four octahedral nanoparticle clusters. The parameters and coefficient of determination of the linear fit are shown below the line.

SI References

1. A. Kotani and S. Shin, *Rev. Mod. Phys.*, 2001, **73**, 203–246.
2. B. C. Bukowski, S. C. Purdy, E. C. Wegener, Z. Wu, A. Jeremy Kropf, G. Zhang, J. T. Miller and J. Greeley, *Physical Chemistry Chemical Physics*, 2023, **25**, 11216–11226.
3. V. J. Cybulskis, B. C. Bukowski, H. T. Tseng, J. R. Gallagher, Z. Wu, E. Wegener, A. J. Kropf, B. Ravel, F. H. Ribeiro, J. Greeley and J. T. Miller, *ACS Catalysis*, 2017, **7**, 4173–4181.